Industrial Crops & Products 191 (2023) 115927

Contents lists available at ScienceDirect

Industrial Crops & Products

journal homepage: www.elsevier.com/locate/indcrop

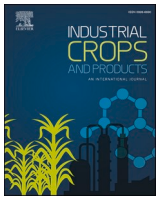

Study of subcritical water scale-up from laboratory to pilot system for brewer's spent grain valorization

P. Alonso-Riaño *, C. Ramos, E. Trigueros, S. Beltrán, M.T. Sanz

Department of Biotechnology and Food Science, University of Burgos, Plaza Misael Bañuelos s/n, 09001 Burgos, Spain

ARTICLE INFO

Keywords:
Subcritical water treatment
Scale-up
Carbohydrates
Protein
Phenolic compounds
Brewer's spent grain

ABSTRACT

The feasibility of an industrial-scale subcritical water (SW) system by scaling up from laboratory to pilot scale in a discontinuous operation mode has been investigated regarding the valorization of brewer's spent grain (BSG). The subcritical water treatment (SWT) of BSG at the pilot scale in a discontinuous mode at 170 °C and 22 min, resulted in the release of 56% of the total carbohydrates present in the BSG. A total pentose yield of 78% was achieved (18% as monomer and 82% as oligomer). The concentration of inhibitors in the hydrolysate was relatively low, 0.22 g/L, 0.31 g/L, and 0.13 g/L of furfural and acetic and formic acids respectively. Other high-value compounds were obtained, such as 6.5 g peptides/L (64% protein yield), 21 mg free amino acids/g protein (2.17% aa yield), and a total phenolic content (TPC) of 17.84 mg GAE/g dry BSG. In general, the results showed good reproducibility when scaling up from laboratory to pilot SW process. Good reproducibility of the scale-up was found for the release yield of arabinoxylo-oligomers, and gluco-oligomers from BSG, also for the protein yield and the release of free amino acids. However, the xylo-oligomers yield was 13% higher at the lab scale than at the pilot scale and higher concentrations of monomers and phenolic compounds were found in the SW hydrolysates obtained at the lab scale. Differences in the preheating time in both systems seem to have an effect on the hydrolysis yield of some the biopolymers. SWT modified the composition of the residual solid, as a decrease in the concentration of hemicellulose and an increase in the glucan content was observed, which may enhance the digestibility of the solid improving a further enzymatic release of glucose from the remaining solid.

1. Introduction

Nowadays, efforts are being made to move towards a more sustainable economy with better use of natural resources and a reduction of greenhouse gas emissions. The development of sustainable biorefineries will contribute to the transition from an economy based on fossil feedstocks to a biobased economy. The use of biomass as raw material opens the possibility to obtain different products and energy through new biorefineries based on a sustainable economy. For that, good quality and low-cost biomass availability and the development of innovative and environmentally friendly technologies for its valorization, are key aspects to implement the bioeconomy (Manzanares, 2020).

Regarding the biomass, brewery spent grain (BSG) is a second-generation biomass based on non-food lignocellulosic biomass generated in the brewing industry in large quantities at low cost. Around 38.6 million metric tons of BSG are annually globally generated from the brewing industry (Kavalopoulos et al., 2021). Due to its high humidity (∽80%) and fermentable sugar content, BSG is susceptible to microbial growth and deteriorates quickly (around 7–10 days) (Bachmann et al., 2022). Hence, BSG is commonly discarded in landfills, used for cattle feed, or incinerated. Nevertheless, BSG is a sustainable resource of valuable biocompounds based on its chemical composition: 12–26%, cellulose, 19–42% hemicellulose, 12–28% lignin, 14–31% proteins, and 3–13% lipids, all expressed on a dry weight basis (Lynch et al., 2016). BSG is also an excellent source of bioactive ingredients such as phenolic compounds, mainly hydroxycinnamic acids (p-coumaric, ferulic, sinapic, and caffeic acids) as well as vitamins and minerals (Ikram et al., 2017). Therefore, BSG valorization in a biorefinery is a powerful strategy, not only from an economic point of view, but also from an environmental perspective (William G. Ampese et al., 2021).

An integral valorization of biomass requires extraction and fractionation of its building blocks including extractives, lipids, proteins, and structural components of the biomass (cellulose, hemicellulose, and lignin). Different treatments have been applied to BSG in the conversion of this biomass into different bio-based products, such as chemical treatment by acid, alkali, or acid-alkali, supercritical fluids, pulsed

* Corresponding author.
E-mail address: pariano@ubu.es (P. Alonso-Riaño).

https://doi.org/10.1016/j.indcrop.2022.115927
Received 1 September 2022; Received in revised form 29 October 2022; Accepted 4 November 2022
Available online 12 November 2022

electric, hydrothermal, and enzymatic hydrolysis (Sganzerla et al., 2021). Among these techniques, subcritical water treatment is a low-cost and environmentally friendly process as no chemicals are required. This technique applies water above its normal boiling point at a pressure high enough to maintain its liquid state and under subcritical conditions (critical point 374 °C and 22.1 MPa). Under these conditions, the physical and chemical properties of water, including its dielectric constant and solubility, vary with temperature, resulting in certain extraction improvement due to the high diffusivity, low viscosity, low surface tension, and higher polarizability. The ionization constant of water gradually increases with temperature, producing more acidic hydronium ions (H_3O^+) and alkaline hydroxide ions (OH^-). In addition, the contribution of H_3O^+ generated by the ionization of the acetyl groups present in hemicelluloses may promote the depolymerization process of polysaccharides (Cocero et al., 2018).

In a SW system, temperature and reaction time are the most important parameters to be considered. The higher the temperature and reaction time, the greater hemicellulose solubilization is achieved; although, if these two variables are too high, hemicellulose sugars and oligomers start to degrade producing inhibitors such as furfural, derived from pentoses, and hydroxymethylfurfural (HMF), derived from hexoses (Cocero et al., 2018). Middle temperatures (175–190 ºC) and short treatment times (15–60 min) enhance the production of oligosaccharides, while longer treatment times (60–120 min) and lower temperatures (160–175 ºC) may lead to a high yield of monosaccharides (Yue et al., 2022).

The utilization of hydrothermal technologies such as SW may be a promising alternative to produce different concentrated sugars from BSG in an industrial plant, but it is still rarely explored (Sganzerla et al., 2021). Especially, considering that most of the studies regarding the use of BSG as source of several valuable bioproducts have been performed at laboratory scale with no consideration for their feasibility and processing costs in pilot and/or industrial plants. Furthermore, most of the studies found in the literature focused only on one product production. Nevertheless, to make full use of the feedstock, enhancing the feasibility of biomass processing, an integral valorization of the raw material should be integrated. Among the different compounds produced by SWT, oligosaccharides attract extensive attention in food, cosmetics, agriculture, pharmacy, and biomedicine (Yue et al., 2022). As reported in the literature, SWT at 170 ºC for 20 min in a batch reactor enabled the production of oligosaccharides from BSG, maintaining the generation of acetic acid and the sugar degradation products quite low (Carvalheiro, 2004). In addition, when hemicellulose is solubilized from the biomass after SWT, most of the cellulose and lignin remain in the solid fraction, which can be submitted to saccharification and fermentation to produce second generation ethanol (Chen et al., 2021). Moreover, SWT has been found to be able to extract/hydrolyze up to 78% of the protein fraction from BSG in a semi-continuous fixed bed reactor at 180 ºC, producing hydrolysates with high antioxidant capacity, as well as phenolic compounds, such as vanillin and p-coumaric and ferulic acids, and a minor amount of free amino acids, mainly aspartic acid (Alonso-Riaño et al., 2021). However, in that work, the concentration of HMF and furfural in the hydrolysates were significantly higher at 185 ºC than at 160 ºC, while the concentration of free amino acids and hydroxycinnamic acids were higher at 160 ºC, suggesting that some of the valuable compounds of BSG are labile at 185 ºC. Therefore, a SW temperature of 170 °C was chosen to carry out the experiments in this work, mainly focused on the release of oligosaccharides from the hemicellulose fraction of BSG, but also considering other valuable biocompounds, while maintaining a relatively low concentration of degradation products.

The main novelty of this work is the SWT scale-up study of BSG from a lab to a pilot plant system considering the main valuable compounds present in the BSG, namely carbohydrates, released as monomer and oligomers, protein and free amino acids, phenolic compounds, the presence of inhibitors, such as acetic acid, furfural, and HMF, as well as the potential uses of the SW solid residue after treatment under a holistic approach. Accordingly, the purposes of this work were: (1) to perform a detailed characterization of the liquid and solid streams generated after the SW process, at different reaction times, at laboratory and pilot scales, (2) to evaluate the reproducibility of the results obtained when scaling up from laboratory to pilot subcritical water process.

2. Experimental section

2.1. Raw material

The BSG was kindly supplied by San Miguel S.A with an initial average humidity of 85% (w/w). This raw material was first preconditioned by washing it and drying in an air convection oven at 45 °C until reaching a final moisture content of 8% (w/w). Dry BSG was milled in a Retsch SM100 mill to get a final fineness lower than 0.5 mm, according to the requirements of the pilot scale plant, by using a bottom sieve with an aperture size of 0.5 mm. The fraction with particle size lower than 0.5 mm was selected and the particle size distribution was determined by a vibratory sieve shaker (CISA, RP.09). Table 1 collects the particle size distribution of the BSG as received (raw BSG), together with the fraction of milled BSG selected for this work.

The selected fraction of BSG (called BSG from now on for simplification) was characterized following the NREL protocols (Sluiter et al., 2010) to determine structural carbohydrates (cellulose and hemicellulose), lignin, moisture, total solids, ash, total extractives, and protein as detailed elsewhere (Alonso-Riaño et al., 2021).

Starch and β-Glucan contents were determined by using the total starch (amyloglucosidase/α-amylase method) and the mixed linkage β-glucan assay kits, respectively, according to the manufacturer's (Megazyme International Ltd.) instructions. The lipid content of the BSG was determined by Soxhlet extraction (Buchi B-8111) using hexane as solvent. Cellulose was estimated as the difference between glucose determined after hydrolysis and glucose due to starch and β-glucans. Hemicellulose was estimated from the arabinoxylans and acetyl groups content in the biomass determined according to the NREL protocols (Sluiter et al., 2010). Extractives-free BSG was submitted to a two-step acid hydrolysis to hydrolyse cellulose and hemicellulose into monosaccharides: (1) 72% (w/w) H_2SO_4, 30 °C, 1 h and (2) 4% (w/w) H_2SO_4, autoclaved at 121 °C for 1 h. Monosaccharides have been determined by HPLC as has been described in Section 2.3.1.

2.2. Subcritical water equipment

2.2.1. Laboratory-scale assay

Subcritical water experiments at the laboratory-scale level were carried out in a lab-built discontinuous reactor (see Fig. 1).

The total capacity of the high-pressure stainless-steel vessel was 0.5 L. Pressurization of the vessel was performed with nitrogen gas. To reach the working temperature, the reactor was covered by a ceramic heating jacket (230 V, 4000 W, ø 95 cm, 160 mm height). A Pt100 sensor, connected to a PID system and placed inside the reactor, allowed to control and register the temperature during the extraction. A needle valve (Autoclave Engineers) followed by a cooling system was connected to collect samples along the assay.

In a typical run, dry BSG was loaded into the reactor and filled with

Table 1
Particle size distribution of BSG as received (raw BSG) and the fraction of BSG selected after milling.

Particle size (mm)	Raw BSG (%)	Selected BSG (%)
> 1	5.19	—
1 – 0.5	52.49	—
0.5 – 0.25	28.45	68.93
0.25 – 0.125	8.69	22.98
< 0.125	1.73	8.09

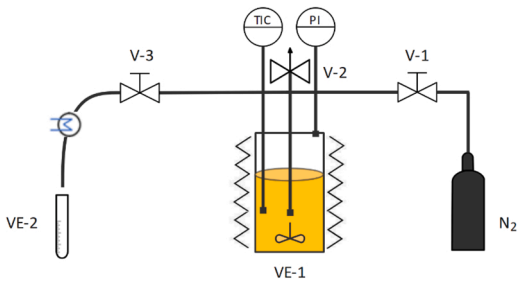

Fig. 1. Diagram of laboratory-scale subcritical water equipment. VE-1: extractor; VE-2: sample collector; V-1: vent valve; V-2: pressure relief valve; V-3: needle valve.

water at a biomass to distilled water ratio of 1:20, corresponding to a biomass loading of 5% (w/v) on a dry weight basis. The working temperature was set at 170 °C, the agitation rate at 500 rpm, and the extraction pressure at 5 MPa and all were maintained during the process. Extraction/hydrolysis kinetics were followed by withdrawing samples through a sampling pipe provided with a metallic filter to avoid the clogging of the pipe. After 60 min the extraction vessel was cooled and, when the temperature was lower than 100 °C, it was depressurized. The temperature inside the rector was registered from the beginning (ambient temperature) until it was cooled down below 100 °C after the treatment (cooling stage). Samples were stored at − 18 °C until analysis.

2.2.2. Pilot-scale assay

SW experiments at pilot-scale level were performed at Hiperbaric's facilities (https://www.hiperbaric.com/es/) by using a discontinuous system with a volume scale factor of 50.

The prototype was mainly composed of a vessel of 25 L capacity, a steam boiler as the heating system, a pump to recirculate and homogenize the biomass inside the reactor, a heat exchanger to avoid cooling during the recirculation process, and a solid/liquid separation system (see Fig. 2). The maximum specifications of the system were 185 °C and 2 MPa. A software built by Hiperbaric was used to execute the operation and control of the process.

The experiments were performed as follows. Firstly, all the system was pre-heated at 80 °C by heating water up to 80 °C in the steam boiler and circulating it through the heat exchanger. Then, the system was totally drained, and the BSG was loaded into the reactor. After that, the reactor was filled with the pressurized water, and the desired temperature was reached by the steam boiler system. Nitrogen gas was used to pressurize the system. At this moment, the recirculation pump was turned on to improve external mass transfer in the extraction/hydrolysis process. The maximum specifications of the pump were a solid concentration of 40% (*w/v*) with a maximum particle size of 0.5 mm, which determined the particle size of the biomass to be used, as mentioned above. A heat exchanger was placed in the recirculation pipe to permit contact with the steam boiler outlet pipe, avoiding heat loss in the recirculation process. A sampling system inserted at the base of the reactor, allowed periodical sampling to follow the extraction/hydrolysis kinetics. At the end of the treatment, the liquid stream was separated from the solid residue by employing a filtration tank.

Experiments were carried out at 5% (*w/v*) biomass loading, temperature of 170 °C and a working pressure of 2 MPa. The treatment time was established from the results obtained in the laboratory-scale assay.

2.3. Analytical methods

2.3.1. Carbohydrate fraction and its degradation products in liquid streams

Monosaccharides and their degradation products were determined by HPLC as described by Alonso-Riaño et al. (2021). The HPLC equipment mainly consists of a Biorad Aminex-HPX-87 H column and its corresponding pre-column and two detectors, a variable wavelength detector (VWD), and a refractive index detector (RID). Sulfuric acid (0.005 M) was the mobile phase. The column and the refractive index detector were maintained at 40 °C. Samples (10 μL) were injected after being filtered through a 0.2 μm syringe filter. Sugars, acetic, and formic acid were quantified by RID while 5-hydroxymethyl-2-furaldehyde (HMF), and furfural were determined by VWD at 284 and 275 nm, respectively. Calibration was performed with pure standards of xylose, arabinose, glucose, and furfural (99%), purchased from Sigma-Aldrich, HMF (97%) from Alfa Aesar, formic acid (98%) from Fluka and acetic acid (99.8%) from VWR.

The monomeric yield was evaluated as the ratio of the amount of sugar monomer released to the medium over the maximum potential yield of sugar obtained from the BSG composition, according to Eq. (1):

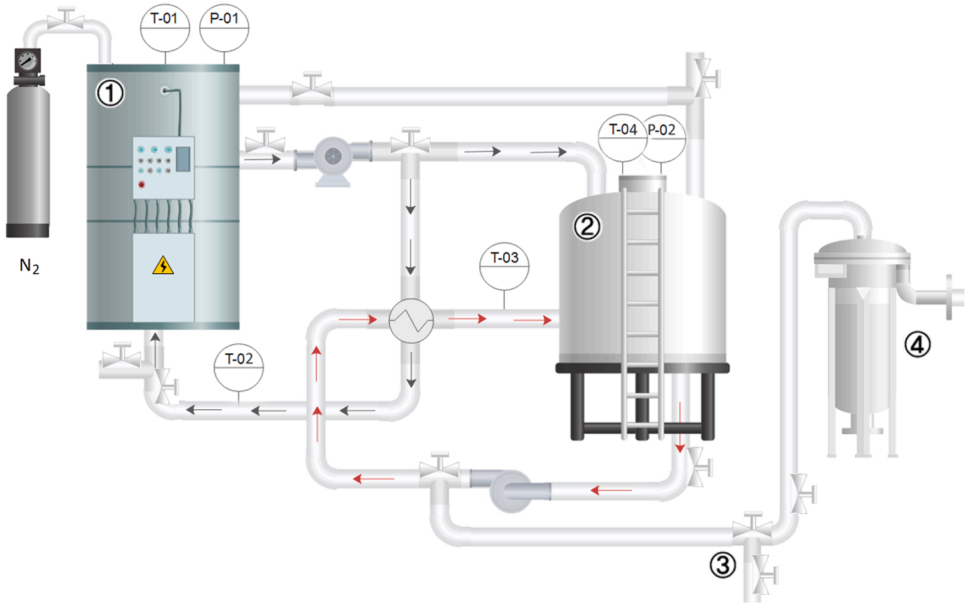

Fig. 2. Diagram of pilot-scale subcritical water plant designed and built in Hiperbaric. 1: boiler preheater and water tank; 2: 25 L extractor; 3: liquid sample collector; 4: filtration tank.

$$\text{Monomeric yield } (\%) = \frac{\text{Monomeric sugar in the hydrolysate}}{\text{Sugar in the raw material}} \cdot 100 \quad (1)$$

Total sugars were determined after an acid hydrolysis step to release monomeric sugars from oligomers for quantification following the NRLE protocols (Sluiter et al., 2006). Total yield of each sugar was determined according to Eq. (2).

$$\text{Total yield } (\%) = \frac{\text{Monomeric and oligomeric sugar in the hydrolysate}}{\text{Sugar in the raw material}} \cdot 100 \quad (2)$$

Oligomer yield was calculated by difference between total and monomer yield.

2.3.2. Protein and free amino acids

Total protein content was determined from the nitrogen content measured by using a TOC/TN analyzer (Shimadzu TOC-V CSN analyzer) using KNO_3 as standard after applying a nitrogen factor of 6.25.

Free amino acids were determined by using the EZ:faast Phenomenex procedure as described by Alonso Riaño et al. (2021).

2.3.3. Total organic carbon

Total carbon and inorganic carbon were measured with a TOC Analyzer Shimadzu (TOC-V CSN model) coupled with an automatic injector (ASI-V model), by using $C_6H_{14}(COOK)(COOH)$, $NaHCO_3$ and Na_2CO_3 as standards. Total organic carbon (TOC) was calculated by subtracting the inorganic carbon from total carbon content.

2.3.4. Phenolic compounds

Total Phenolic Content (TPC) was determined by using the Folin–Ciocalteu reagent following the method described by Singleton et al. (1999). A calibration curve was prepared with standard solutions of gallic acid by following the same colorimetric method, and results were expressed as mg of gallic acid equivalent (GAE) per gram of dry BSG.

Individual phenolic compounds were identified and quantified according to the method previously described by Alonso-Riaño et al. (2020). The sample was filtered through a 0.2 μm syringe filter. After that, 80 μL of sample were injected in the HPLC system. The separation was performed at 25 °C on a Kinetex® μm Biphenyl 100 Å, 250 × 4.6 mm column (Phenomenex). The mobile phase consisted of ammonium acetate 5 mM with acetic acid (1%; v/v) in water (solvent A) and ammonium acetate 5 mM with acetic acid (1%; v/v) in acetonitrile (solvent B). The composition of the mobile phase varied during the run according to a nonlinear gradient as follows: from 0 to 7 min, 2% of solvent B (isocratic); from 7 to 20 min, from 2% to 8% solvent B; from 20 to 35 min, from 8% to 10% solvent B and from 35 to 55 min, from 10% to 18% solvent B and post time of 10 min, at a flow rate of 0.8 mL/min. Detection and quantification were performed at 240, 280, 330, 340, 350, and 370 nm. The HP ChemStation software was employed to collect and analyze the chromatographic data delivered by the diode array detector and our own library was used to identify the different phenolic compounds by comparing retention times and spectral data with those of authentic standards: syringic aldehyde, protocatechuic aldehyde, vanillin, p-coumaric acid, ferulic acid, catechin, vanillic acid, 4-vinylphenol and 4-vinylguaicol standards (Sigma-Aldrich). Peak purity was checked to exclude any contribution from interfering peaks. Individual stock solutions of the above phenolic compounds, and their mixtures, were prepared in methanol to plot the calibration curves.

2.3.5. Elemental composition

Elemental composition (C, H, N, S) of raw material and solid residue after SWT was determined by an organic elemental micro-analyzer equipment (Thermo Scientific Model Flash 2000). Oxygen content was determined by difference. The high heating value (HHV) of BSG and the solid remaining after SWT was evaluated according to Eq. (3) (Friedl et al., 2005):

$$HHV\ (kJ/kg) = 3.55C^2 - 232C - 2230H + 51.2C{\cdot}H + 131N + 20600 \quad (3)$$

2.4. Statistical analysis

All values were expressed as mean ± standard deviation from triplicate measurements. The significance of the differences was determined based on an analysis of the variance with the Fisher's Least Significant Difference (LSD) method at p-value ≤ 0.05 using the Statgraphics X64 software. Error bars in all graphs are 95% confidence intervals.

3. Results and discussion

3.1. BSG characterization

The chemical composition of the BSG employed in this work is presented in Table 2, on a weight percentage dry basis. Carbohydrates represent up to 50% of the BSG dry weight, comprising xylan (21.6%), glucan (19.1%), and arabinan (9.5%). The cellulose and hemicellulose content of the BSG used in this work was 14% and 32%, respectively. Besides carbohydrates, the BSG also contained a significant amount of protein (22.1% *w/w)* and lignin (20.8% *w/w*), and minor amounts of lipids, ash, starch, and β-glucans.

Extractives in water and in ethanol (water-insoluble), containing non-structural compounds, accounted for 9.2% and 5.3%, with a TPC of 3.65 and 1.09 mg GAE/g dry BSG, respectively. The protein content in water and ethanol extractives, determined by the TN content and applying the factor 6.25, was 5.53% and 0.51%, respectively. However, according to Qin et al. (2018)., the value of total nitrogen in the sample might include non-protein nitrogen compounds, such as free amino acids degraded from protein during the mashing process. These authors reported a protein yield of 64–66% from BSG in water at 60 °C for 24 h. In the present work, the amount of crude protein in water extractives (5.53%) accounted for 25% of the BSG total protein. This value agrees with values reported in the literature for this type of biomass

Table 2
Chemical composition of the selected fraction of BSG (particle size < 0.5 mm) expressed in weight percentage on a dry basis.

Component	Composition of selected BSG (%)
Extractives in water	9.2 ± 0.1
TOC	6.08 ± 0.06
Protein	5.53 ± 0.01
TPC	0.365 ± 0.009
Extractives in ethanol	5.3 ± 0.1
Protein	0.513 ± 0.004
TPC	0.109 ± 0.004
Total Protein[a]	22.1 ± 0.5
Glucan content	19.1 ± 0.2
Cellulose	14.0 ± 0.2
Starch	4.11 ± 0.06
β-Glucan	0.99 ± 0.01
Hemicellulose content	32.0 ± 0.6
Xylan	21.6 ± 0.4
Arabinan	9.5 ± 0.4
Acetyl groups	0.93 ± 0.05
Lignin	20.8 ± 0.2
Acid Soluble lignin	5.3 ± 0.2
Acid Insoluble lignin	15.5 ± 0.1
Lipids	6.2 ± 0.3
Ash	3.32 ± 0.06

Values are expressed as mean ± standard deviation from triplicate determination.

[a] Total Protein includes the protein content in the extractives fraction (6.08%).

(Alonso-Riaño et al., 2021; Arauzo et al., 2019). Total organic carbon in water extractives was also determined, corresponding to 6.08% on a dry weight basis.

3.2. Heating rate

Temperature profiles for the SW experiments performed at lab- and pilot-scale are shown in Fig. 3.

Different heating rates were observed for both systems. Specifically, the time needed to reach the desired working temperature, 170 °C, was 15.7 min at lab-scale, while it was achieved after only 4.5 min when SWT was performed in the pilot plant, since water was fed into the pilot plant reactor at 80 °C. It is worth describing the differences between the temperature profiles in as much detail as possible since heating rate influences the results regarding the biocompounds release from BSG. The pre-heating time was defined as the time needed to reach the working temperature. From now on, the time when the working temperature was reached will be referred to as time 0, which will be the beginning of the isothermal period. In each system, two different heating rates were observed, being faster at the beginning. The initial heating rate at pilot-scale was 83.4 °C/min, decreasing down to 13.4 °C/min after 3 min, whereas the heating rate at lab-scale was 14.4 °C/min for the first 10 min, with a reduction after that down to 5.3 °C/min. According to the literature, the heating time to achieve the desired reaction temperature in SW ranges from 15 to 80 min, and heating rates vary from 2° to 7.1°C/min (Rodríguez et al., 2021). Therefore, the heating rate in the pilot system was noticeably higher than the previous reported values in literature. Furthermore, the average operating temperature during the isothermal period was 174 ± 3 °C and 171 ± 3 °C at lab- and pilot-scale, respectively.

Additionally, it must be highlighted that cooling was almost instantaneous at pilot-scale, while it took about 60 min to decrease the temperature below 100 °C inside the reactor at lab-scale. Therefore, considering the three stages, pre-heating time, isothermal time, and cooling time, the total time that the solid was in contact with water at a temperature higher than 100 °C was 115 min at lab-scale for a defined isothermal time of 45 min. In contrast, experiments performed at pilot-scale could be considered under isothermal operation as both, the pre-heating and the cooling periods were truly short. The combined effect of temperature and reaction time during hydrothermal processes was evaluated by the severity factor parameter according to Eq. (4):

$$R_o = t \cdot \exp\left(\frac{T-100}{14.75}\right) \quad (4)$$

where R_0 is the severity factor, t is the treatment time (min), T is the operating temperature (°C), T_{ref} is 100 °C because under this temperature no significant solubilization nor depolymerization of the hemicellulose take place, and the value 14.75 is a typical activation energy for glycosidic bond cleavage of carbohydrates under hydrothermal treatment assuming conversion is first order. The severity factor is commonly determined considering only the isothermal stage and expressed as $S_0 = \log R_0$, being in this case, 3.83 (45 min, 174 °C) and 3.43 (22 min, 171 °C) for lab- and pilot-scale, respectively. However, the severity factor can be modified to incorporate the effect of the non-isothermal stages by integrating the temperature vs. time profile along the heating, isothermal, and cooling periods (Ruiz et al., 2021; Wang et al., 2016).

$$R_o = R_{o,Heating} + R_{o,Isothermal} + R_{o,Cooling} = \int_{t_0}^{t_H} \exp\left(\frac{T(t)-100}{14.75}\right)\cdot dt + t\cdot\exp\left(\frac{T-100}{14.75}\right) + \int_{t_F}^{t_C}\left(\frac{T(t)-100}{14.75}\right)\cdot dt \quad (5)$$

where T (t) is the function of temperature vs. time determined from the temperature profile at each stage, being T = 7.30•t + 58.09 and T = 0.98•t + 230.21 the T ptofiles obtained at lab-scale for the heating and cooling stages, respectively. t_0-t_H is the time range used to reach the work temperature, T, from 100 °C (9.04 min), t is the isothermal time (45 min) and t_F-t_C is the time range used to decrease temperature from T to 100 °C after the isothermal period (61.87 min). The severity factor of the treatment at lab-scale calculated according to Eq. (5), increased up to 7.47 by considering the three stages during the hydrothermal process. Nevertheless, this value should be used with caution to compare the results with those reported in the literature for two reasons: (1) the severity factor is often calculated in the literature only for the isothermal period even if higher heating times were employed and (2) this value should be used only to compare the composition of the residual solid, since samples from the liquid stream were collected periodically through the sampling pipe, and in this case, the stage of cooling time was not considered.

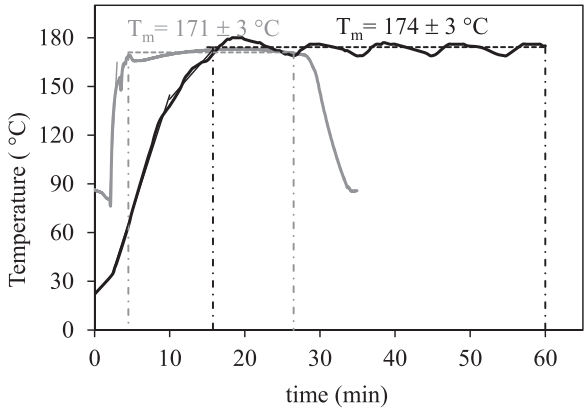

Fig. 3. Hydrothermal temperature profile during subW treatment performed at lab-scale, continuous black lines (—), and at pilot-scale, continuous grey lines (—). Discontinuous lines delimit the isothermal period in each system. T_m: medium temperature during the isothermal period.

3.3. Carbohydrate fraction extraction/hydrolysis

Fig. 4(a) shows the release kinetics of glucose, xylose, and arabinose monomers in the laboratory-scale extracts (LSE) and the pilot-scale extracts (PSE) from BSG. Fig. 4(b) shows total sugars (released as monomers and oligomers) expressed as monomer equivalent.

Additionally, the individual sugar yield in each system, obtained at different reaction times as monomer and as oligomer (expressed as monomer equivalent) has been represented in Fig. 5.

During the preheating time (15.7 min for laboratory-scale and 4.5 min for pilot-scale) a fraction of the sugars, mainly in oligomeric form, was released. At that time, glucose, xylose, and arabinose equivalent concentrations were 1.41 g/L, 1.55 g/L, and 1.27 g/L, respectively, in LSE and 1.46 g/L, 1.29 g/L, and 0.36 g/L, respectively, in PSE, released as total sugars (monomers and oligomers). Moreover, arabinose was found as monomer in concentrations of 0.43 g/L and 0.11 g/L in LSE and PSE, respectively, while the amounts of xylose and glucose monomers were negligible in both systems at zero time (time when the selected temperature was reached). Similarly, Vallejos et al. (2015) found that a fraction of hemicellulose was hydrolyzed from sugarcane bagasse during the time needed to reach 170 ºC and Camargos et al. (2021) reported a concentration of arabinose and xylose oligomers of 3.42 g/L in the hydrolysate of BSG treated at 80 °C for 10 min, which probably were not covalently bonded to the BSG structure.

As expected, the release of monomeric sugars was lower than oligomeric sugars for both systems, since SW, with no acid addition, produces mostly oligomers with minor amounts of monomers, being necessary a lower pH to hydrolyse most of the hemicellulose into monomers (Mosier et al., 2005). Monomeric arabinose content in PSE increased with time up to 1.83 g/L at the end of the assay (22 min), while a higher concentration of arabinose, 2.57 g/L, was found in LSE at

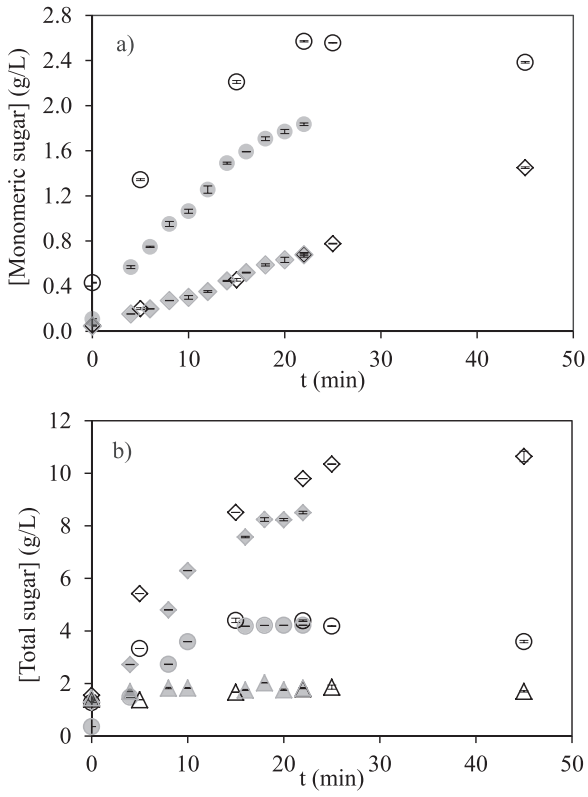

Fig. 4. Sugar concentration in subW extracts released as **(a)** monomers: xylose (◇, ◆) and arabinose (○, ●) and **(b)** as total sugars (monomer + oligomer): xylose (◇, ◆) and arabinose (○, ●), and as gluco-oligomers (△, ▲) along assays performed at laboratory-scale (open symbols) and at pilot-scale (full symbols).

the same time (see Fig. 4a), probably due to the higher pre-heating time needed in this system. After that, arabinose concentration decreased due to the formation of degradation products, mainly furfural. As can be seen in Fig. 6(a), furfural concentration increased from 0.27 g/L to 0.73 g/L in the range-time from 22 to 45 min in LSE while slightly lower concentration of furfural, 0.20 g/L, was found in PSE at 22 min

This notwithstanding, the arabinose content in PSE after 22 min of treatment was slightly higher (3.98 g/100 g dry BSG) than the highest value of 3.1 g arabinose/100 g dry BSG reported by Torres-Mayanga et al. (2019) in a semicontinuous reactor, employing a flow rate of 10 mL/min, with 112 g water/g BSG and 180 °C (log $R_0 = 3.32$), while higher furfural content was reported by these authors in the hydrolysates, 1.2 g/100 g BSG.

Regarding total arabinose, similar amounts were released in both systems, reaching a plateau after around 15 min of treatment for both of then, as can be seen in Fig. 4(b). Although the total arabinose yield was not significantly different in both systems (at 5% signification), the monomer/oligomer ratio was higher in LSE than in PSE. The arabinose yield obtained in monomeric and in oligomeric form in each system can be seen in Fig. 5(c) and (f). High hydrolysis yields were achieved for both systems, reaching values close to 90%. As previously describe at laboratory scale, arabinose degradation was observed at time longer than 22 min

The concentration of xylose, both in monomeric and oligomeric forms, increased with time in the experiments carried out in both systems, reaching a maximum concentration of total xylose of 10.64 g/L, corresponding to 94% yield and a monomeric xylose concentration of 1.45 g/L (12.8% yield) in LSE after 45 min of treatment. After 22 min of treatment a total xylose yield of 87% was achieved in LSE, being slightly lower in PSE, 75%. Although the highest xylose yield was obtained at the highest time assayed, the concentration of degradation compounds was noticeably higher **(**Fig. 6**)**. In this period (22–45 min), furfural concentration increased from 0.27 g/L to 0.73 g/L, acetic acid concentration increased from 0.32 to 0.64 g/L and formic acid concentration increased from 0.07 to 0.15 g/L. Therefore, increasing time of treatment resulted in furfural formation as dehydration product of pentoses (C5) sugars and small amounts of HMF from glucose (C6) sugar. Degradation of these compounds produces formic acid, acetic acid and levulinic acid. These compounds are strong inhibitors of fermentation (Vanmarcke et al., 2021), therefore, their formation should be avoided if subsequent fermentation of the SW hydrolysates is planned. However, acetic acid was mainly released due to deacetylation of the hemicellulose fraction.

As can be seen in Fig. 6(b) the formation of acetic acid was similar in laboratory-scale and in pilot-scale during the first 22 min of extraction, suggesting that hemicellulose deacetylation occurred parallelly in both systems. Notwithstanding, pentosan yield (as total xylose + total arabinose) was higher in laboratory scale (87%) than in pilot-scale (78%). According to Cocero et al. (2018), hemicellulose hydrothermal fractionation comprises numerous physical phenomena such as hemicellulose cleaving into decreasing molecular weight oligomers, hemicellulose deacetylation, hemicelluloses dissolution and mass transfer between the solid and the liquid, production of sugars and sugars degradation into furfural or other compounds. The results obtained in this work suggested that production of sugars and sugars degradation into furfural occurred earlier in laboratory-scale than in pilot-scale, probably due to the higher preheating time needed to reach the work temperature. According to Rodríguez et al. (2021) the main factor of discrepancies within different hydrothermal studies performed under the same conditions lies in the preheating time, being necessary to study the treatment under rigorous isothermal operation to successful scale up from laboratory to pilot plant. On the other hand, pressure was higher in the laboratory assay (5 MPa) than in pilot-scale (2 MPa). A recent study about the influence of pressure (2.5 and 10 MPa) on the release of the main components of sugarcane bagasse (SCB), during hydrothermal treatment in a continuous flow mode, showed that the monomer xylose yield was similar at both pressures considered (22 mg/g xylan) being also similar the content of reducing sugars and total reducing sugars at both pressures. In addition, the yield of xylooligomers with a degree of polymerization between 2 and 6 at 10 MPa was 27% higher than that obtained at 2.5 MPa (87.53 and 111.39 mg/g xylan at 2.5 and 10 MPa, respectively). These results suggest that the pressure may exert an effect on the degree of polymerization of the oligomers released by SWT, since the xylan chains subjected to higher pressure (10 MPa) may suffer hydrolysis to a greater extent than those subjected to 2.5 MPa (Monteiro et al., 2022). However, it is well known that pressure has very little influence on the properties of water, as long as the water remains in the liquid state (Cocero et al., 2018; Plaza and Turner, 2015). In this sense, (Mayanga-Torres et al. (2017) found that the effect of increasing the pressure from 22.5 to 30 MPa on the reducing sugars and total reducing sugars yields obtained by subcritical water hydrolysis from coffee industry residues was not significant.

Regarding glucose, it was not detected as monomer in any of the systems. Consequently, small concentrations of HMF were found in the SW extracts, indicating that probably, small amounts of glucose monomer were released and quickly dehydrated to produce HMF. Levulinic acid was not detected in the SW extracts, as it comes from HMF degradation. The concentration profile of gluco-oligomers was similar in the extracts collected at different times in both systems, reaching a maximum level of 1.86 g/L and 2.03 g/L in LSE (25 min) and in PES (18 min), respectively. Gluco-oligomers were not released from the cellulosic fraction. As can be seen in Tables 2, 26.7% of glucans were non-cellulosic glucans. They mainly came from starch, which is easily hydrolyzed during the subcritical water treatment, while the cellulosic fraction was not hydrolyzed under the subcritical water conditions

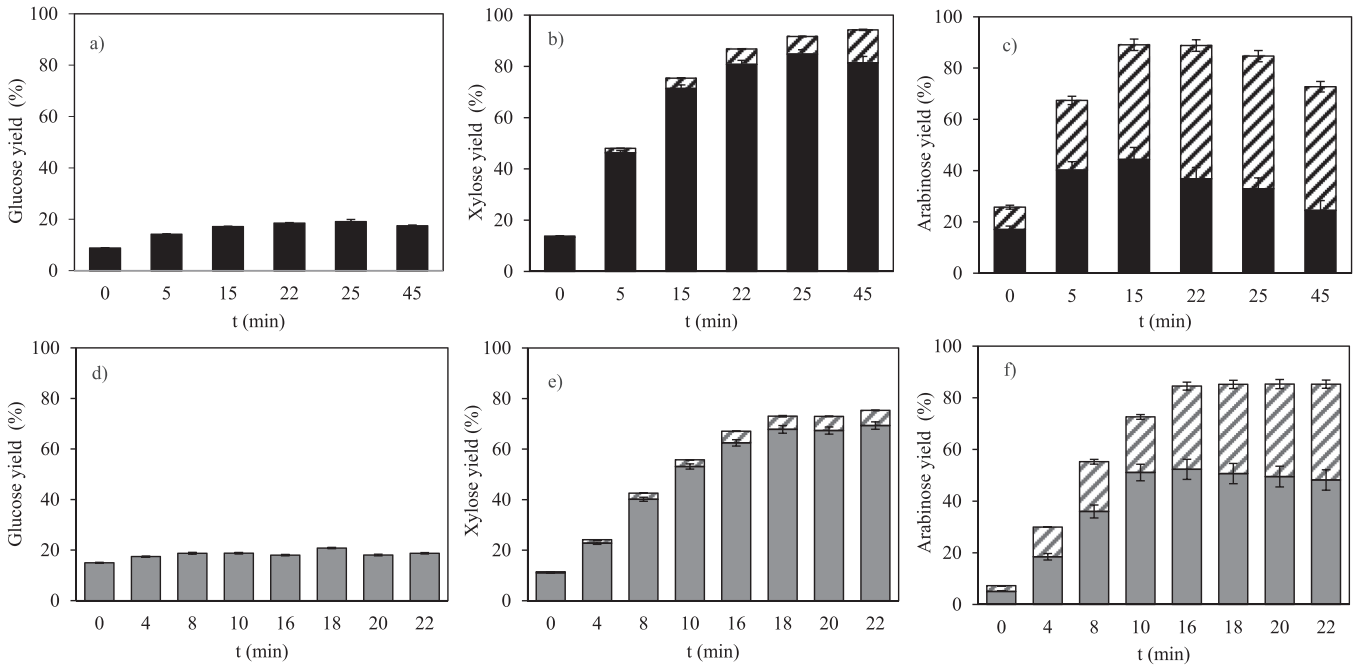

Fig. 5. Sugar yield in subcritical water extracts from BSG collected at the different time intervals as oligomers (■, ■) and monomers (▨, ▨) at laboratory-scale (black): (a) glucose, (b) xylose and (c) arabinose, and at pilot-scale (grey): (d) glucose (e) xylose and (f), arabinose at 170 °C.

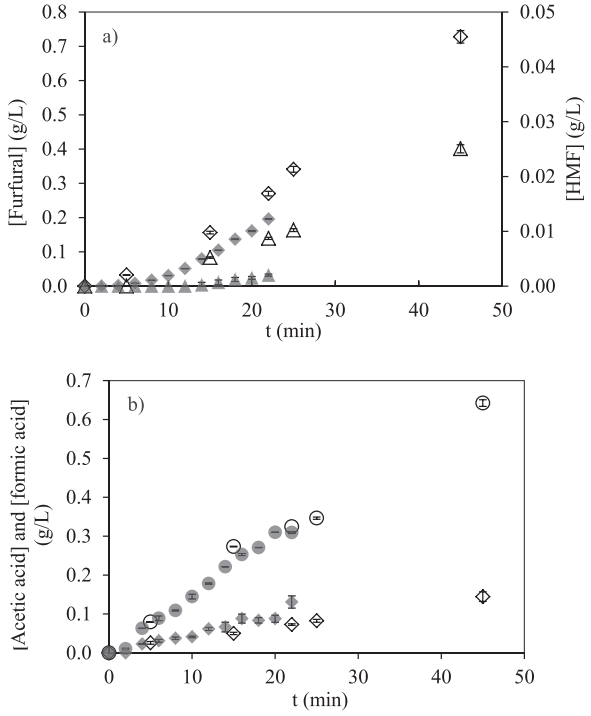

Fig. 6. Concentration of sugar-derived compounds **(a)** furfural (◇, ◆) and hydroxymethylfurfural, HMF (△, ▲) and **(b)** acetic acid (○, ●) and formic acid (◇, ◆) in subW extracts collected along assays performed at laboratory-scale (open symbols) and at pilot-scale (full symbols).

performed on this work (Deguchi et al., 2008). Consequently, the maximum yields of gluco-oligomers obtained in laboratory and in pilot scale were 19.07% and 20.8%, respectively, (see Fig. 5(a) and (d)).

The results obtained in this work are consistent with those found in the literature. The value of xylan susceptible to be hydrolyzed has been reported for the hydrothermal treatment for different biomasses, such as sugarcane bagasse with a high fraction of hydrolyzed xylan, 92% (Vallejos et al., 2015) and 85–89% (Garrote et al., 2001) and sugar maple with percentage of hydrolyzed xylan in the range from 78% to 87% (Mittal et al., 2009). All these results indicate that a high fraction of the total amount of xylans present in the solid are susceptible to hydrolysis by SW from different biomass.

Likewise, Carvalheiro (2004) reported that the release of monomeric xylose from BSG by SW at 170 °C, and a liquid/solid ratio of 8 g/g, increased with reaction time (for a total treatment time of 60 min), whereas the maximal concentration of free arabinose was obtained after 20 min. The amount of solubilized xylan reported by these authors was 84–90% (from 150° to 190°C) while arabinan was almost completely solubilized. On the other hand, the maximum percentages of soluble saccharides, xylooligosaccharides (XOS) and xylose, recovered from xylan, in the temperature range studied by these authors, were lower (53–72%) and were reached after 20 min of treatment when working at 170 °C, decreasing, after that, the XOS recovery. In the present work, higher xylan recovery was achieved at pilot and laboratory scales after 22 min, 75% and 87%, respectively, increasing the latest up to 94% at the longest time assayed (45 min). The decrease of xylo-oligosaccharides yield at times greater than 20 min reported by these authors, may be explained by the higher pre-heating time employed in that work (32–44 min to reach working temperatures between 150 and 190 °C) as a high initial concentration of xylooligomers (11.08 g/L) in the hydrolysates was reported, suggesting that the hydrolysis of the hemicellulose started during the pre-heating time. Moreover, the higher yield of total xylose obtained in the present work, could be explained by the better heat and mass transfer achieved by operating at higher liquid/solid ratio and by reducing the biomass

particle size by milling.

3.4. Protein fraction extraction/hydrolysis

Protein content was determined as the total nitrogen content in SW extracts per 100 g of dry BSG, after applying the nitrogen factor 6.25. The kinetics of protein extraction/hydrolysis obtained at laboratory and pilot scales have been represented in Fig. 7, together with the protein yield. At the beginning of the isothermal treatment, 2.10 ± 0.03 and 5.33 ± 0.05 g protein/100 g dry BSG were found in PSE and LSE, respectively.

As mentioned above, BSG water-soluble protein accounted for 5.53% (*w/w*). Thus, the results indicated that almost all the soluble protein fraction was extracted during the preheating time at laboratory-scale assay, while a fraction of water-soluble protein remained unextracted at time 0 min when the assay was performed at pilot-scale. After 22 min of treatment, protein content in LSE and PSE were 13.95 and 14.14 g/100 g dry BSG, respectively, corresponding to protein yields of 63 ± 2% and 64 ± 2%, respectively. Despite these minor differences in the curves of the release of protein fraction between both systems, there was no significant difference between protein yield after 22 min of treatment between the two systems (p-value < 0.05). Therefore, the release of protein in SW showed great reproducibility at different scales. Furthermore, when time increased from 22 min to 45 min at lab-scale, the value of protein yield (66 ± 3%) was not statistically different than that obtained at 22 min (p-value < 0.05), suggesting a temperature limitation of the protein release. According to Lamp et al. (2020), this fact may be due to two reasons: (1) a limitation of the protein solubility due to the SW polarity, which remains constant at each temperature, while a temperature increase, associated to a decrease in the SW polarity, could lead to an increase in protein solubility, and (2) higher activity energies of hydrolysis for some peptide bonds, which require elevated temperatures to be broken. Higher protein yield (78%) was achieved from BSG by SW extraction at 185 °C in a semi-continuous fixed-bed reactor in a previous work (Alonso-Riaño et al., 2021). However, protein concentration in SW extracts was greater in this work (6.5 g/L) than that obtained when operating in semi-continuous mode at 185 °C and a flowrate of 4 mL/min, accumulated after 4 h of treatment (1.7 g/L). Furthermore, the protein yield reached in this work was higher than those obtained by other hydrolytic methods such as enzymatic hydrolysis (47.1%, 6% protease, 4 h), alkaline hydrolysis (50.5%, 0.1 M NaOH, 4 h) (Alonso-Riaño et al., 2021) or ultrasound-assisted extraction (UAE) (46.6%, water, 50 °C, 30 min) (Alonso-Riaño et al., 2020). The results obtained in this work were in good agreement with those reported in the literature. For instance, Lamp at al. (Lamp et al., 2020) found that protein solubilization started at 89 °C, achieving the highest protein yield in the hydrolysate (75%) at 170 °C and 20 min when studying the protein recovery from the insoluble fraction of stillage by SW at different temperatures and times (110–210 °C for 10–90 min).

Likewise, a minor fraction of the protein content was hydrolysed as free amino acids in the SW extracts. Free amino acids in SW extracts were determined by the sum of individual free amino acids measured by gas chromatography, as has been plotted in Fig. 8.

The amount of free amino acids present in the SW extracts obtained by both systems, around 21 mg free amino acids/g protein, after 22 min of treatment, was not significantly different. After that, the concentration of free amino acids in LSE slightly increased up to 23.8 ± 0.5 mg free amino acids/g protein at 45 min, although the difference of this value with that obtained at 22 min was not statistically significant ($p < 0.05$).

The release curves for individual amino acids by SW at lab and pilot-scale systems have been represented in Fig. 9, grouped into non-polar (Fig. 9(a) and (b)) and polar amino acids (Fig. 9(c) and (d)).

The concentration of non-polar amino acids in PSE and LSE increased or remained constant when increasing time. Conversely, a concentration decrease of some polar amino acids along time was observed in the time range studied in this work. Specifically, glutamic acid showed a noticeable concentration decrease after 5 min of treatment in both systems. Glutamic acid has been reported as one of the most labile amino acids since it lactamizes with temperature to form pyroglutamic acid (Abdelmoez et al., 2007). In general, according to Lamp et al. (2020), the constant rate of degradation for the polar amino acids is about one order of magnitude higher than for the non-polar amino acids, taking place at 170 °C for almost all polar amino acids. Furthermore, polar amino acids present a high tendency to undergo Maillard reactions with carbonyl groups or reducing carbohydrates that have been released during SWT.

Table 3 shows free amino acid yields, calculated as the ratio of individual amino acids found in the extracts and in the raw material. Free amino acids yields obtained in this work, around 2.1% after 22 min of extraction in both systems, were lower than those obtained from BSG in a semi-continuous reactor, accumulated after 4 h of SWT, at different temperatures (125–185 °C), which varied from 2.9% at 125 °C to the maximum level, 5.5%, obtained at 160 °C (Alonso-Riaño et al., 2021). In that work, a remarkable derease of amino acids yield was observed when increasing temperature up to 185 °C, and was related to polar amino acids degradation at severity factor conditions higher than 3.2. Among all the amino acids, aspartic acid showed by far the highest yield in both systems, 19% in laboratory-scale and 21% in pilot-scale after 22 min of treatment, exhibiting a decrease until 19% when reaction time increased up to 45 min

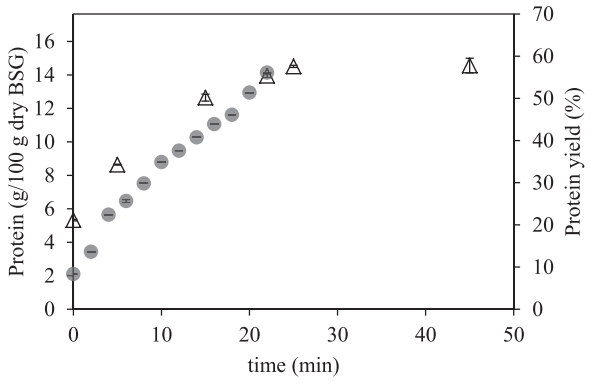

Fig. 7. Protein content, expressed as g per 100 g of dry BSG and protein yield in SW extracts obtained along time at lab-scale (△) and at pilot-scale (●).

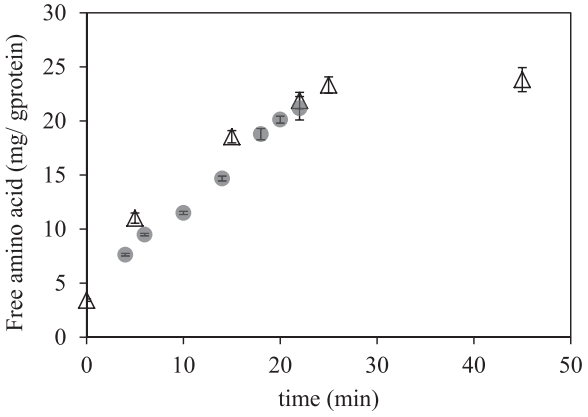

Fig. 8. Free amino acids, expressed as mg per g of protein in dry BSG, in subcritical water extracts obtained along time at lab-scale (△) and pilot-scale (●).

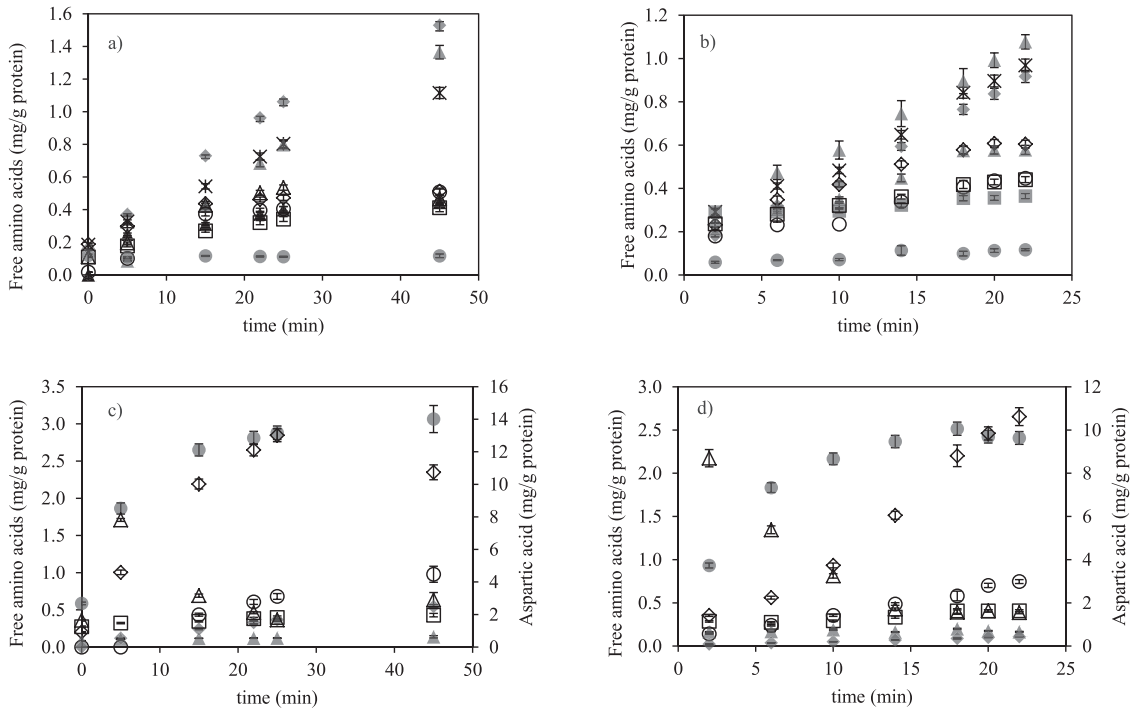

Fig. 9. Accumulative formation of individual amino acids. Non-polar amino acids **(a)** at lab-scale **(b)** at pilot-scale (* alanine, ◆ glycine, ▲ valine, △ leucine, ○ isoleucine, ◇ proline, ◇ phenylalanine, □ methionine and ● tryptophan). Polar amino acids **(c)** at lab-scale **(d)** at pilot-scale (● lysine, ○ serine, △ glutamic acid, ◇ histidine, ◇ aspartic acid, ◆ threonine and ▲ tyrosine). (Experimental data includes standard deviations, $n = 3$ technical replicates).

3.5. Polyphenolic compounds

3.5.1. Total polyphenol content in SW extracts

Total phenolic content (TPC) in LSE and PSE was determined by the Folin-Ciocalteu method and has been represented at different treatment times in Fig. 10.

The difference between both systems was noticeable. In the lab-scale system, the initial phenolic content was 6.27 mg GAE/g dry BSG and increased with time up to a TPC of 34 mg GAE/g dry BSG after 45 min of isothermal treatment. This TPC in LSE was 38% higher than in PSE, suggesting that the higher preheating time at lab-scale determined higher TPC at the same isothermal time of treatment in both systems.

Table 3
Amino acid profile of BSG and free amino acid yields in the SW extracts obtained in pilot-scale at 22 min and in lab-scale at 22 and 45 min, expressed as mg free amino acids/g protein and percent yield as the ratio of individual amino acids in the extracts and in the raw material.

Amino acid	BSG	Pilot-Scale SWE, 22 min		Lab-Scale SWE 22 min		Lab-Scale SWE 45 min	
	mg/g protein	mg/g protein	Yield (%)	mg/g protein	Yield (%)	mg/g protein	Yield (%)
Alanine	61 ± 2	0.97 ± 0.03^{b}	1.59 ± 0.07	0.72 ± 0.02^{a}	1.19 ± 0.05	1.11 ± 0.03^{c}	1.83 ± 0.08
Aspartic acid	57 ± 2	10.6 ± 0.4^{a}	19 ± 1	12.1 ± 0.4^{b}	21 ± 1	10.7 ± 0.5^{a}	19 ± 1
Glutamic acid	97 ± 3	0.41 ± 0.01^{a}	0.42 ± 0.02	0.46 ± 0.01^{a,b}	0.48 ± 0.02	0.63 ± 0.10^{b}	0.65 ± 0.11
Glycine	48 ± 1	0.92 ± 0.03^{a}	1.92 ± 0.08	0.96 ± 0.03^{a}	2.01 ± 0.09	1.53 ± 0.05^{b}	3.19 ± 0.14
Histidine^{e}	30 ± 1	0.41 ± 0.01^{a}	1.37 ± 0.07	0.38 ± 0.02^{a}	1.28 ± 0.08	0.43 ± 0.02^{a}	1.44 ± 0.10
Hydroxylysine	6 ± 2	n.d.	-	n.d.	-	n.d.	-
Hydroxyproline	7.8 ± 0.2	n.d.	-	n.d.	-	0.34 ± 0.01^{a}	4.3 ± 0.2
Isoleucine^{e}	76 ± 2	0.45 ± 0.02^{a}	0.59 ± 0.03	0.40 ± 0.01^{a}	0.52 ± 0.02	0.51 ± 0.02^{b}	0.67 ± 0.03
Leucine^{e}	87 ± 3	0.58 ± 0.02^{b}	0.67 ± 0.03	0.50 ± 0.01^{a}	0.58 ± 0.03	0.47 ± 0.02^{a}	0.54 ± 0.03
Lysine^{e}	67 ± 2	2.41 ± 0.07^{a}	3.6 ± 0.2	2.81 ± 0.03^{b}	4.2 ± 0.2	3.1 ± 0.2^{b}	4.6 ± 0.3
Methionine^{e}	25.3 ± 0.8	0.36 ± 0.01^{a}	1.40 ± 0.06	0.37 ± 0.02^{a}	1.47 ± 0.08	0.44 ± 0.01^{b}	1.76 ± 0.08
Phenylalnine^{e}	76 ± 3	0.44 ± 0.01^{b}	0.58 ± 0.02	0.32 ± 0.01^{a}	0.42 ± 0.02	0.41 ± 0.02^{b}	0.54 ± 0.04
Proline	137 ± 4	0.60 ± 0.02^{c}	0.44 ± 0.02	0.46 ± 0.02^{a}	0.34 ± 0.02	0.51 ± 0.02^{b}	0.38 ± 0.02
Serine	22.1 ± 0.7	0.75 ± 0.02^{b}	3.4 ± 0.2	0.61 ± 0.04^{a}	2.70 ± 0.18	1.0 ± 0.1^{c}	4.4 ± 0.5
Threonine^{e}	30 ± 1	0.43 ± 0.01^{b}	1.40 ± 0.06	0.33 ± 0.02^{a}	1.08 ± 0.07	0.54 ± 0.03^{c}	1.79 ± 0.10
Tryptophan^{e}	11.2 ± 0.3	0.12 ± 0.02^{a}	1.00 ± 0.05	0.113 ± 0.004^{a}	1.01 ± 0.04	0.12 ± 0.01^{a}	1.04 ± 0.11
Tyrosine	24 ± 1	0.66 ± 0.02^{b}	2.8 ± 0.1	0.54 ± 0.02^{a}	2.3 ± 0.3	0.63 ± 0.04^{b}	2.7 ± 0.2
Valine^{e}	141 ± 4	1.08 ± 0.03^{b}	0.76 ± 0.03	0.68 ± 0.02^{a}	0.48 ± 0.02	1.36 ± 0.04^{c}	0.97 ± 0.04
TAA	1002 ± 9	21.2 ± 0.4^{a}	2.11 ± 0.05	21.8 ± 0.4^{a}	2.17 ± 0.04	23.8 ± 0.5^{a}	2.38 ± 0.06
TEAA	543 ± 7	6.3 ± 0.1^{a}	1.15 ± 0.02	5.9 ± 0.1^{a}	1.09 ± 0.02	7.4 ± 0.2^{a}	1.35 ± 0.04
TEAA/TAA (%)	54.2 ± 0.8^{b}	30 ± 1^{a}		27.1 ± 0.5^{a}		31 ± 1^{a}	

n.d., not detected. TAA, total amino acids. TEAA, total essential amino acids. TEAA/TAA: ratio of essential amino acids to total amino acids. Values are expressed as mean ± standard deviation from triplicate determination. Values with different letters in each column are significantly different when applying the Fisher's least significant differences (LSD) method ($p \leq 0.05$) for mg aa/$g_{protein}$ values. Aspartic acid includes asparagine. Glutamic acid includes glutamine.

The color of the hydrolysates became darker by increasing time, being darker those obtained at lab scale than at pilot scale, considering the same isothermal time. This color change would indicate the formation of brown pigments in Maillard reactions.

In a previous work about the release of phenolic compounds from BSG in a semi-continuous SW extractor, in the temperature range from 125 °C to 185 °C (Alonso-Riaño et al., 2021), it was found that 23.01 mg GAE/g dry BSG and 33.03 mg GAE/g dry BSG were obtained by the Folin–Ciocalteu method, at 160 °C and 185 °C, accumulated after 240 min of SWT, at a flow rate of 4 mL/min. Thus, the TPC in LSE after 45 min of treatment was comparable with the highest TPC obtained in that study. In this previous study, higher release of hydroxycinnamic acids was found at 160 °C than at 185 °C. According to Fabian et al. (2010), the optimal temperature for the extraction of coumaric and ferulic acids from defatted rice bran was 175 °C, decreasing at higher temperatures because thermal decomposition of these compounds started at around 172 °C. In this work, p-coumaric acid, ferulic acid and vanillin were found in both PSE and LSE and the kinetic curves of the release of these compounds has been represented in Fig. 11.

The same trend than for TPC was observed for the release of the identified phenolic compounds. The concentration of these compounds increased along time in both systems, being higher in LSE than in PSE after 22 min of treatment. At this moment, the amounts of p-coumaric acid, ferulic acid and vanillin were 20%, 17% and 14% higher in LSE than in PSE, respectively. The maximum concentration of p-coumaric acid, ferulic acid and vanillin were 272 ± 1 μg/g dry BSG, 365.1 ± 0.9 μg/g dry BSG and 439.7 ± 0.4 μg/g dry BSG, respectively achieved in LSE at the highest time studied, 45 min. Moreover, other phenolic compounds were also identified in LSE after 45 min of treatment, such as protocatechuic aldehyde (65 ± 3 μg/g dry BSG), catechin (72 ± 3 μg/g dry BSG), vanillic acid (25.0 ± 0.4 μg/g dry BSG) and 4-vinylguaiacol (90 ± 2 μg/g dry BSG), coming the last one from the thermal decarboxylation of ferulic acid (Zago et al., 2022). Therefore, the total amount of phenolic compounds identified in LSE after 45 min of treatment was 1.38 mg/g dry BSG, a value remarkable lower than 34 mg GAE/g dry BSG, as determined by the Foilin-Ciocalteu assay. The great difference between these values could be explained by different facts. On the one hand, some individual phenolic compounds could not be properly identified by our system due to lack of standards. For instance, together with phenolic acids, several isomeric ferulate dehydrodimers and one dehydrotrimer have been reported as components of the BSG matrix (Moreira et al., 2012). On the other hand, compounds related to Maillard reactions, such as protein-carbohydrate conjugates, melanoidins, and heterocyclic compounds may interfere in the TPC determination by the Folin-Ciocalteu assay, being possible to consider HMF and furfural as indicators of these reactions (Alonso-Riaño et al., 2021).

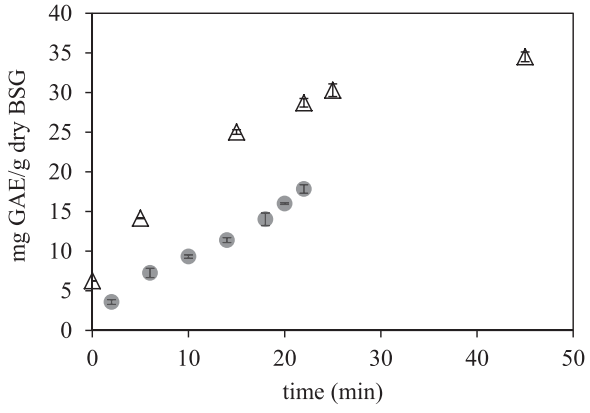

Fig. 10. Total phenolic content, expressed as mg of GAE per g of dry BSG in lab-scale extracts (△) and pilot-scale extracts (●), released from BSG, along time.

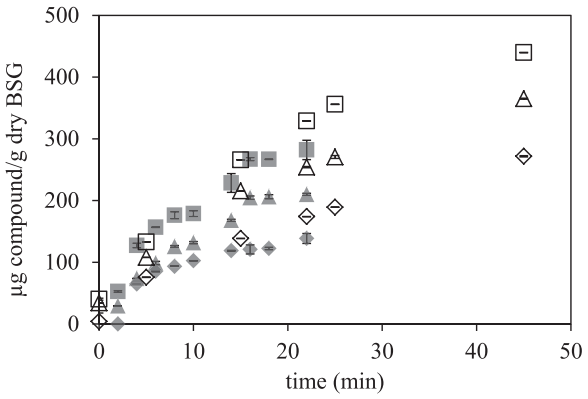

Fig. 11. Accumulative individual phenolic compounds released from BSG at pilot-scale (open symbols) and lab-scale (full symbols): p-coumaric acid (◇, ◆), ferulic acid (△, ▲) and vanillin (◇, ■).

3.6. Organic carbon in the subcritical water extracts

The total organic carbon (TOC) present in the SW extracts obtained at laboratory and pilot scales has been plotted in Fig. 12.

TOC extraction yield increased with time; although, after 25 min of isothermal extraction at lab-scale, a plateau was reached. The same trend in the release of TOC was observed for the release of other biocompounds: a higher initial value in the LSE than in PSE at the beginning of isothermal treatment, due to the release of some compounds from milled BSG that were water-soluble or easily hydrolysable during the pre-heating time. This behavior suggests that these compounds were not linked to the cell-wall polysaccharide matrix. Specifically, the amount of TOC at time 0 in LSE, 6.21%, was in good agreement whit TOC in water extractives 6.08% in a dry weight basis.

The extraction rates of both systems were evaluated in each lineal range, from 0 to 25 min at lab-scale and for all time range studied at pilot-scale (0–22 min). There were not statistically significant differences among the slopes at the 90% or higher confidence level, while there were statistically significant differences among the intercepts at the 99% confidence level.

TOC includes all the C containing biocompounds described previously, including polysaccharides, peptides and in a lesser extent

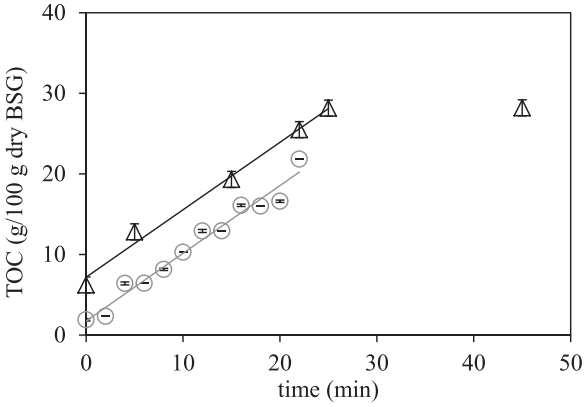

Fig. 12. TOC content in subcritical water extracts collected in subcritical water extracts obtained along time at lab-scale (△) and pilot-scale (○). Lines represent the extraction/hydrolysis rate of TOC in the lineal range at lab-scale: TOC = 0.8365 time + 7.178, R^2 = 0.9902 and at pilot-scale: TOC = 0.8397 time + 7.1740, R^2 = 0.9696.

phenolic compounds and free amino acids. According to these results, most of the soluble C compounds found in subW hydrolysates would correspond to polysaccharides and peptides. Therefore, future work should be carried out to fractionate these two biocompounds. In this regard, a sequential ultrafiltration process for oligosaccharide and peptide fractionation from a macroalgae subcritical water hydrolysate has been recently published (Trigueros et al., 2022). These authors proposed sequential ultrafiltration steps with different cut-off sized membranes (100, 5 and 1 kDa), obtaining a sum of retentates with more than 90 wt% of the total oligosaccharide fraction present in the SW hydrolysate and a final permeate with a purity index towards peptides close to 71 wt%.

3.7. Solid residue after SWT

The solid residue obtained after the subcritical water treatment was characterized in the same way as the initial feedstock, according to NREL protocols. The results of these characterizations are shown in Table 4.

After SWT at lab-scale, 43.5% of solids were recovered, whereas the amount of solid that remained after the SWT at pilot plant scale could not be properly determined, due to the difficulty of a complete recovery. The total extraction yield at lab-scale was 56.5%, evaluated according to Eq. (6):

$$Yield \quad (\%) = \frac{W - W_i}{W} \cdot 100 \tag{6}$$

where w is the weight of the dry BSG placed into the reactor and w_i is the weight of the washed and dry solid residue remaining after the SWT.

In the two systems studied, the concentration of glucans increased in the residue with respect to the composition of the initial feedstock, due to the solubilization of other components and the fact that cellulose is not hydrolysed in subcritical water, as discussed above. The presence of glucose in the hydrolysates is derived mainly from the solubilization of starch, as can be seen in the reduction of the starch content from 4.11% in the raw BSG to 0.22% determined in PSWR. In addition, an increase of insoluble lignin was observed in both residues, which confirmed that this fraction of the biomass was not released under SWT. The insoluble lignin to soluble lignin ratio is a parameter indicative of the effects of heat treatment in BSG (de Camargos et al., 2021). This ratio was 3.3 and 2.1-fold higher in the residue obtained in the laboratory and in the pilot plant respectively, compared to the ratio in the raw BSG, suggesting that the heat treatment caused changes in the chemical structure of lignin.

Table 4
Chemical composition of solid residues remained after SWT of BSG performed at lab-scale (LSWR) and at pilot-scale (PSWR).

Compound	LSWR (% dwb)	PSWR (% dwb)
Glucans	34.7 ± 0.6 [b]	30.2 ± 0.4 [a]
Starch	Not determined	0.22 ± 0.02
Cellulose	34.7 ± 0.6 [b]	30.0 ± 0.4 [a]
Hemicellulose	2.3 ± 0.5 [a]	14.9 ± 0.3 [b]
Xylan	2.31 ± 0.06 [a]	11.7 ± 0.2 [b]
Arabinan	Not detected	2.7 ± 0.2
Acetate	Not detected	0.56 ± 0.02
Lignin	47.1 ± 0.4 [b]	40 ± 1 [a]
Acid insoluble lignin	42.7 ± 0.4 [b]	35 ± 1 [a]
Acid soluble lignin	4.4 ± 0.1 [a]	5.6 ± 0.1 [b]
Protein	12.3 ± 0.1 [a]	16.2 ± 0.7 [b]
Ash	2.71 ± 0.01 [a]	2.77 ± 0.09 [a]
Yield (% dwb)	56.5	Not determined

Values are expressed as mean ± standard deviation from triplicate determination. Values with different letters in each raw (a or b) are significantly different when applying the Fisher's least significant differences (LSD) method at p-value ≤ 0.05.

The increase in the proportion of glucans and insoluble lignin in the residues was more pronounced in the residue from the laboratory assay, due to the higher severity conditions employed in this experiment (see Section 3.2). When SWT was performed at lab-scale, almost total solubilization of the hemicellulose was observed, remaining a small proportion of xylans in the residue, 2.31 ± 0.06%, while arabinans and acetyl groups were not detected. The cellulose/hemicellulose ratio in the original BSG was 0.44, while after SW hydrolysis this ratio increased up to 15 and 2 in LSWR and PSWR, respectively. Furthermore, the protein content was reduced from 22.1 ± 0.1%, initially present in the BSG, to 12.3 ± 0.1% and 15.7 ± 0.1% in LSWR and PSWR, respectively, due to the protein solubilization by the SWT.

The elemental composition of the solid residues after extraction was collected in Table 5.

The carbon content (C) in LSWR and PSWR was higher than in BSG, while no significant differences were found between the values obtained in both residues. The oxygen content (O) was not affected by the SWT; however, the molar ratio O:C was significantly lower after SW at lab-scale than in feedstock, which is associated with a decrease in the amount of OH, carboxyl (COOH) and carbonyl (C═O) groups. Additionally, the decrease of both, nitrogen content (N) and molar ratio N:C in the solid was observed when increased the severity of the treatment.

Slightly higher HHV values were obtained for the residual solid in both systems compared to the raw BSG, although no significant differences were determined between the solid residue obtained in the pilot plant and the raw BSG.

Table 6. shows the mass balance obtained for the different components of BSG determined in this work after the SWT performed at lab scale. The feed mass, m_{feed}, of each compound has been calculated from the chemical composition of the BSG and the initial amount of BSG charged into the reactor (Table 2). The outlet mass of each component was evaluated considering the remaining amount in the solid residue after cooling the extractor and washing the solid (Tables 4 and 5) and the amount of each compound present in the LSE after 45 min of isothermal treatment. The mass balance for each compound was calculated according to Eq. (7):

$$Mass\ balance,\ MB\ (\%) = \frac{Compound_{outlet}\ (g)}{\text{Compound}_{feed}\ (g)} \cdot 100 \tag{7}$$

In general, mass balances present deviations lower than 10%, which can be considered acceptable mass balance errors for hydrothermal treatments of a complex matrix such as BSG, specially, considering the long time of the cooling stage. As expected, the highest MB deviation was observed for arabinan balance, which is in concordance with the degradation of arabinose that was observed from 22 min of treatment (Fig. 4). At this regard, the arabinan mass loss observed, 2.62 g, would contribute to a furfural production of 1.90 g, while 1.6 g were formed

Table 5
Elemental analysis, ash content, H:C, O:C and N:C molar ratios and estimated heating value (HHV) of BSG and the solid residues remained after SWT performed at lab-scale (LSWR) and at pilot-scale (PSWR).

Compound	BSG	LSWR	PSWR
C (% dwb)	49.2 ± 0.5[a]	52 ± 1[b]	51.3 ± 0.1[b]
H (% dwb)	6.64 ± 0.01[a]	6.9 ± 0.1[b]	6.66 ± 0.06[a,b]
N (% dwb)	3.77 ± 0.01[c]	1.97 ± 0.02[a]	2.8 ± 0.1[b]
O (% dwb)	37.0 ± 0.6[a]	36 ± 1[a]	36.4 ± 0.2[a]
Ash (% dwb)	3.32 ± 0.06[b]	2.71 ± 0.02[a]	2.77 ± 0.09[a]
H:C	1.62 ± 0.02[a]	1.57 ± 0.0 4[a]	1.56 ± 0.01[a]
O:C	0.57 ± 0.01[b]	0.52 ± 0.02[a]	0.532 ± 0.003[a,b]
N:C	0.066 ± 0.002[c]	0.0323 ± 0.0007[a]	0.047 ± 0.002 [b]
HHV (MJ/kg)	20.2 ± 0.3[a]	21.5 ± 0.7[b]	21.1 ± 0.2[a,b]

Values are expressed as mean ± standard deviation from triplicate determination. Values with different letters in each raw (a, b or c) are significantly different when applying the Fisher's least significant differences (LSD) method (p-value ≤ 0.05).

Table 6
Mass balance of SWT performed at lab-scale from 100 g of dry BSG.

Compound	m_{feed} (g)	m_{outlet} (g)	MB (%)
Solid	100	43.5	-
Glucan	19.1 ± 0.2	18.4 ± 0.3	96 ± 1
Xylan	21.6 ± 0.4	21.4 ± 0.4	99 ± 2
Arabinan	9.5 ± 0.4	6.88 ± 0.09	73 ± 3
Acetic acid[1]	0.95 ± 0.04	1.40 ± 0.03	148 ± 6
Lignin	20.8 ± 0.2	20.5 ± 0.2	99 ± 1
AIL	15.5 ± 0.1	18.6 ± 0.2	120 ± 1
ASL	5.3 ± 0.2	1.93 ± 0.06	36 ± 1
C	49.2 ± 0.5	51.0 ± 0.9	104 ± 1
N	3.53 ± 0.08	3.19 ± 0.07	90 ± 2

"AIL" and "ASL" stand for acid insoluble lignin and acid soluble lignin, respectively. Values are expressed as mean ± standard deviation from triplicate determination. (1) Acetic acid mass in feed was calculated from acetyl groups present in the BSG.

after 45 min of isothermal treatment. However, the concentration of furfural increased to 1.5 g/L (3.3 g/100 g dry BSG) during the cooling time (data not shown), indicating that not only arabinan but also xylan underwent degradation along this period. In addition, the value of MB corresponding to acetic acid, noticeably higher than 100, suggests that acetic acid was formed not only from the deacetylation of acetyl groups present in BSG hemicellulose but also from the degradation of other compounds such as amino acids, among others. Regarding amino acids, their degradation under hydrothermal conditions could be followed in different pathways such as decarboxylation to produce carbonic acid and amines, and deamination to produce ammonia and organic acids. The results suggested that the second pathway was major as a mass loss was observed for N but not for C. Moreover, the higher amount of aspartic acid found in the SW extracts, together with its high rate of degradation by a predominant deamination mechanism, was consistent with the loss of N (Sato et al., 2004). As described by Lamp et al. (2020) volatile degradation products associated to the Maillard reaction (e.g., pyrroles, pyridines, imidazoles, pyrazines, oxasoles, thiazoles or aldol condensation products) could be also smelled as "a typical coffee-like aroma" during reactor depressurization after SWT. These authors reported a total mass loss inside the reactor of 25% due to the formation of volatile degradation products, at a severity factor of 5.4, while decreasing protein yield.

On the other hand, MB fitted well for total lignin; but was over and under 100 for acid insoluble lignin and acid soluble lignin, respectively, suggesting that changes in the lignin structure took place during the SWT. According to the literature, hydrothermal treatment may cause condensation reactions and structural alteration in the lignin, while lignin droplets have been observed on the surface of the treated solid (Zhuang et al., 2016).

This work was focused on comparison of the release of different biocompounds at lab and pilot plant scale. For that purpose the composition of the liquid hydrolysate as well as for the remaining solid after treatment has been deeply discussed. However, a future study about the energy efficiency of the subcritical water process applied to BSG treatment will be useful for process scaling-up into the industrial scale. In this regard, some technoeconomic studies in continuous and discontinuous subcritical water reactors to obtain different products, from different biomasses, have been found in the literature. For instance, in a techno-economic study of the SWT to produce sugars from BSG at 160 °C, in a flow-through reactor of 500 L the heat required for the reactor was reported as 610 kJ/kg (Sganzerla et al., 2021). These authors concluded that a high amount of energy was required to operate in a continuous mode and the heat required for an industrial reactor should be optimized. Different studies about SWT as pretreatment for obtaining different bioproducts from different biomasses have been also performed in discontinuous mode (He et al., 2017; Phojaroen et al., 2022; Shaji et al., 2022). A combined hydrothermal-mechanical pretreatment has been reported as an effective pretreatment process to obtain fermentable sugars by enzymatic hydrolysis from corncob. The energy efficiency of the overall process was 28.3 g of fermentable sugars/kWh, being the energy consumption during the SWT (180 °C, 30 min), 16.567 kWh/kg of biomass (59.641 MJ/kg) (Phojaroen et al., 2022). The energy balance for methane production from rice straw pretreated with SW (150 °C, 20 min) resulted in a net energy gain ($\Delta E = E_{outlet} - E_{inlet}$) of 2741 MJ/t (He et al., 2017). The total electricity demand to produce xylitol from sugarcane bagasse pretreated with dilute acid in SW (170 °C, 15 min) was 2779 kW, including the electricity demand for all the unit processes involved in the plant; 72% for fermentation and filtration units, 8.5% for pretreatment and washing units and 9.67% for the evaporation and compressor units. Interestingly, the overall energy balance showed that the total heat content of the solid residue, considering a calorific value of 14.08 MJ/kg, is higher than the energy required to provide the necessary amount of steam in the plant (Shaji et al., 2022). It should be noted that the HHV of the SW pretreated solids obtained in the present work were higher, 21.5 ± 0.7 and 21.1 ± 0.2 MJ/kg for LSWR and PSWR, respectively (**see** Table 5).

4. Conclusions

The results of this preliminary study may contribute to a proper scale-up process from laboratory to pilot system for brewer's spent grain valorization by subcritical water treatment. The study found that there were no significant differences between the two systems for the release of total polysaccharide oligomers, protein yield, or free amino acids release. However, there were differences observed for the release of individual xylo oligomers, with the lab scale system having a 13% higher release yield. There were also significant differences found for the release of monosaccharides and the total phenolic content (TPC) between the two systems. Heating and cooling rates were remarkabely higher at pilot scale. The higher preheating time employed at lab scale seems to have an effect on the TPC and monosaccharides release, while the higher residence time of the solid residue at lab scale greatly affected its chemical composition.

Funding

This work was supported by the Agencia Estatal de Investigación, Spain, [grant numbers PID2019–104950RB-I00 / AEI / 10.13039/501100011033, TED2021–129311B-I00 and PDC2022–133443-I00] and the Junta de Castilla y León (JCyL), Spain and the European Regional Development Fund (ERDF) [grant number BU050P20]. E. Trigueros and P. Alonso-Riaño predoctoral contracts are funded by JCyL and the European Social Fund (ESF) [ORDEN EDU/574/2018 and EDU/556/2019 respectively].

CRediT authorship contribution statement

Patricia Alonso-Riaño: Investigation, Data curation, Writing – original draft preparation, Methodology. **C. Ramos**: Resources, Validation. **E. Trigueros**: Investigation, Methodology. **S. Beltrán**: Conceptualization, Visualization, Writing – review & editing, Funding acquisition. **M. T. Sanz**: Writing – review & editing, Supervision, Project administration, Funding acquisition.

Declaration of Competing Interest

The authors declare that they have no known competing financial interests or personal relationships that could have appeared to influence the work reported in this paper.

Data availability

Data will be made available on request.

Acknowledgments

The authors acknowledge Mahou SA for kindly providing the BSG used in this work and Hiperbaric SA for kindly allowing the use of their facilities.

References

Abdelmoez, W., Nakahasi, T., Yoshida, H., 2007. Amino acid transformation and decomposition in saturated subcritical water conditions. Ind. Eng. Chem. Res 46, 5286–5294. https://doi.org/10.1021/ie070151b.

Alonso-Riaño, P., Diez, M.T.S., Blanco, B., Beltrán, S., Trigueros, E., Benito-Román, O., 2020. Water ultrasound-assisted extraction of polyphenol compounds from brewer's spent grain: Kinetic study, extract characterization, and concentration. Antioxidants 9. https://doi.org/10.3390/antiox9030265.

Alonso-Riaño, P., Sanz, M.T., Benito-Román, O., Beltrán, S., Trigueros, E., 2021. Subcritical water as hydrolytic medium to recover and fractionate the protein fraction and phenolic compounds from craft brewer's spent grain. Food Chem. 351. https://doi.org/10.1016/j.foodchem.2021.129264.

Arauzo, P.J., Du, L., Olszewski, M.P., Meza Zavala, M.F., Alhnidi, M.J., Kruse, A., 2019. Effect of protein during hydrothermal carbonization of brewer's spent grain. Bioresour. Technol. 293, 122117 https://doi.org/10.1016/j.biortech.2019.122117.

Bachmann, S.A.L., Calvete, T., Féris, L.A., 2022. Potential applications of brewery spent grain: Critical an overview. J. Environ. Chem. Eng. https://doi.org/10.1016/j.jece.2021.106951.

de Camargos, A.B., Fonseca, Y.A., da, Silva, N.C.S., Barreto, E., da, S., Adarme, O.F.H., Paranhos, A.G., de, O., Gurgel, L.V.A., Baêta, B.E.L., 2021. Production of biogas and fermentable sugars from spent brewery grains: Evaluation of one- and two-stage thermal pretreatment in an integrated biorefinery. J. Environ. Chem. Eng. 9. https://doi.org/10.1016/j.jece.2021.105960.

Carvalheiro, F., 2004. Production of oligosaccharides by autohydrolysis of brewery's spent grain. Bioresour. Technol. 91, 93–100. https://doi.org/10.1016/S0960-8524(03)00148-2.

Chen, J., Wang, X., Zhang, B., Yang, Y., Song, Y., Zhang, F., Liu, B., Zhou, Y., Yi, Y., Shan, Y., Lü, X., 2021. Integrating enzymatic hydrolysis into subcritical water pretreatment optimization for bioethanol production from wheat straw. Sci. Total Environ. 770. https://doi.org/10.1016/j.scitotenv.2021.145321.

Cocero, M.J., Cabeza, Á., Abad, N., Adamovic, T., Vaquerizo, L., Martínez, C.M., Pazo-Cepeda, M.V., 2018. Understanding biomass fractionation in subcritical & supercritical water. J. Supercrit. Fluids 133, 550–565. https://doi.org/10.1016/j.supflu.2017.08.012.

Deguchi, S., Tsujii, K., Horikoshi, K., 2008. Crystalline-to-amorphous transformation of cellulose in hot and compressed water and its implications for hydrothermal conversion, 191–19 Green. Chem. 10. https://doi.org/10.1039/b713655b.

Fabian, C., Tran-Thi, N.Y., Kasim, N.S., Ju, Y.H., 2010. Release of phenolic acids from defatted rice bran by subcritical water treatment. J. Sci. Food Agric. 90, 2576–2581. https://doi.org/10.1002/jsfa.4123.

Friedl, A., Padouvas, E., Rotter, H., Varmuza, K., 2005. Prediction of heating values of biomass fuel from elemental composition. Anal. Chim. Acta 544, 191–198. https://doi.org/10.1016/j.aca.2005.01.041.

Garrote, G., Domínguez, H., Parajó, J.C., 2001. Kinetic modelling of corncob autohydrolysis. Process Biochem. 36, 571–578. https://doi.org/10.1016/S0032-9592(00)00253-3.

He, L., Huang, H., Zhang, Z., Lei, Z., Lin, B.-L., 2017. Energy recovery from rice straw through hydrothermal pretreatment and subsequent biomethane production. Energy Fuels 31, 10850–10857. https://doi.org/10.1021/acs.energyfuels.7b01392.

Ikram, S., Huang, L., Zhang, H., Wang, J., Yin, M., 2017. Composition and nutrient value proposition of brewers spent grain. J. Food Sci. 82, 2232–2242. https://doi.org/10.1111/1750-3841.13794.

Kavalopoulos, M., Stoumpou, V., Christofi, A., Mai, S., Barampouti, E.M., Moustakas, K., Malamis, D., Loizidou, M., 2021. Sustainable valorisation pathways mitigating environmental pollution from brewers' spent grains. Environ. Pollut. 270. https://doi.org/10.1016/j.envpol.2020.116069.

Lamp, A., Kaltschmitt, M., Lüdtke, O., 2020. Protein recovery from bioethanol stillage by liquid hot water treatment. J. Supercrit. Fluids 155, 104624. https://doi.org/10.1016/j.supflu.2019.104624.

Lynch, K.M., Steffen, E.J., Arendt, E.K., 2016. Brewers' spent grain: a review with an emphasis on food and health. J. Inst. Brew. 122, 553–568. https://doi.org/10.1002/jib.363.

Manzanares, P., 2020. The role of biorefinering research in the development of a modern bioeconomy. Acta Innov. 47–56. https://doi.org/10.32933/ActaInnovations.37.4.

Mayanga-Torres, P.C., Lachos-Perez, D., Rezende, C.A., Prado, J.M., Ma, Z., Tompsett, G. T., Timko, M.T., Forster-Carneiro, T., 2017. Valorization of coffee industry residues by subcritical water hydrolysis: Recovery of sugars and phenolic compounds. J. Supercrit. Fluids 120, 75–85. https://doi.org/10.1016/j.supflu.2016.10.015.

Mittal, A., Chatterjee, S.G., Scott, G.M., Amidon, T.E., 2009. Modeling xylan solubilization during autohydrolysis of sugar maple and aspen wood chips: Reaction kinetics and mass transfer. Chem. Eng. Sci. 64, 3031–3041. https://doi.org/10.1016/j.ces.2009.03.011.

Monteiro, C.R.M., Rodrigues, L.G.G., Cesca, K., Poletto, P., 2022. Evaluation of hydrothermal sugarcane bagasse treatment for the production of xylooligosaccharides in different pressures. J. Food Process Eng. https://doi.org/10.1111/jfpe.13965.

Moreira, M.M., Morais, S., Barros, A.A., Delerue-Matos, C., Guido, L.F., 2012. A novel application of microwave-assisted extraction of polyphenols from brewer's spent grain with HPLC-DAD-MS analysis. Anal. Bioanal. Chem. 403, 1019–1029. https://doi.org/10.1007/s00216-011-5703-y.

Mosier, N., Wyman, C., Dale, B., Elander, R., Lee, Y.Y., Holtzapple, M., Ladisch, M., 2005. Features of promising technologies for pretreatment of lignocellulosic biomass. Bioresour. Technol. 96, 673–686. https://doi.org/10.1016/j.biortech.2004.06.025.

Phojaroen, J., Jiradechakorn, T., Kirdponpattara, S., Sriariyanun, M., Junthip, J., Chuetor, S., 2022. Performance evaluation of combined hydrothermal-mechanical pretreatment of lignocellulosic biomass for enzymatic enhancement. Polym. (Basel) 14, 2313. https://doi.org/10.3390/polym14122313.

Plaza, M., Turner, C., 2015. Pressurized hot water extraction of bioactives. TrAC - Trends Anal. Chem. 71, 39–54. https://doi.org/10.1016/j.trac.2015.02.022.

Qin, F., Johansen, A.Z., Mussatto, S.I., 2018. Evaluation of different pretreatment strategies for protein extraction from brewer's spent grains. Ind. Crops Prod. 125, 443–453. https://doi.org/10.1016/j.indcrop.2018.09.017.

Rodríguez, F., Aguilar-Garnica, E., Santiago-Toribio, A., Sánchez, A., 2021. Polysaccharides release in a laboratory-scale batch hydrothermal pretreatment of wheat straw under rigorous isothermal operation. Molecules 27, 26. https://doi.org/10.3390/molecules27010026.

Ruiz, H.A., Galbe, M., Garrote, G., Ramirez-Gutierrez, D.M., Ximenes, E., Sun, S.N., Lachos-Perez, D., Rodríguez-Jasso, R.M., Sun, R.C., Yang, B., Ladisch, M.R., 2021. Severity factor kinetic model as a strategic parameter of hydrothermal processing (steam explosion and liquid hot water) for biomass fractionation under biorefinery concept. Bioresour. Technol. https://doi.org/10.1016/j.biortech.2021.125961.

Sato, N., Quitain, A.T., Kang, K., Daimon, H., Fujie, K., 2004. Reaction kinetics of amino acid decomposition in high-temperature and high-pressure water. Ind. Eng. Chem. Res 43, 3217–3222. https://doi.org/10.1021/ie020733n.

Sganzerla, W.G., Ampese, L.C., Mussatto, S.I., Forster-Carneiro, T., 2021. A bibliometric analysis on potential uses of brewer's spent grains in a biorefinery for the circular economy transition of the beer industry. Biofuels, Bioprod. Bioref. bbb 2290. https://doi.org/10.1002/bbb.2290.

Sganzerla, W.G, Zabot, G.L., Torres-Mayanga, P.C., Buller, L.S., Mussatto, S.I., Forster-Carneiro, T., 2021. Techno-economic assessment of subcritical water hydrolysis process for sugars production from brewer's spent grains. Ind. Crops Prod. 171. https://doi.org/10.1016/j.indcrop.2021.113836.

Shaji, A., Shastri, Y., Kumar, V., Ranade, V.V., Hindle, N., 2022. Sugarcane bagasse valorization to xylitol: Techno-economic and life cycle assessment. Biofuels, Bioprod. Bioref. 16, 1214–1226. https://doi.org/10.1002/bbb.2368.

Singleton, V.L., Orthofer, R., Lamuela-Raventós, R.M.B.T.-M. in E., 1999. [14] Analysis of total phenols and other oxidation substrates and antioxidants by means of folin-ciocalteu reagent. In: Oxidants and Antioxidants Part A. Academic Press, pp. 152–178. https://doi.org/10.1016/S0076-6879(99)99017-1.

Sluiter, A., Hames, B., Ruiz, R., Scarlata, C., Sluiter, J., Templeton, D., 2006, Determination of Sugars, Byproducts, and Degradation Products in Liquid Fraction Process Samples: Laboratory Analytical Procedure (LAP); Issue Date: 12/08/2006.

Sluiter, J.B., Ruiz, R.O., Scarlata, C.J., Sluiter, A.D., Templeton, D.W., 2010. Compositional analysis of lignocellulosic feedstocks. 1. Review and description of methods. J. Agric. Food Chem. 58, 9043–9053. https://doi.org/10.1021/jf1008023.

Torres-Mayanga, P.C., Azambuja, S.P.H., Tyufekchiev, M., Tompsett, G.A., Timko, M.T., Goldbeck, R., Rostagno, M.A., Forster-Carneiro, T., 2019. Subcritical water hydrolysis of brewer's spent grains: Selective production of hemicellulosic sugars (C-5 sugars). J. Supercrit. Fluids 145, 19–30. https://doi.org/10.1016/j.supflu.2018.11.019.

Trigueros, E., Sanz, M.T., Beltrán, S., Ruiz, M.O., 2022. Filtration of subcritical water hydrolysates from red macroalgae byproducts with ultraporous ceramic membranes for oligosaccharide and peptide fractionation. J. Memb. Sci. 660. https://doi.org/10.1016/J.MEMSCI.2022.120822.

Vallejos, M.E., Felissia, F.E., Kruyeniski, J., Area, M.C., 2015. Kinetic study of the extraction of hemicellulosic carbohydrates from sugarcane bagasse by hot water treatment. Ind. Crops Prod. 67, 1–6. https://doi.org/10.1016/j.indcrop.2014.12.058.

Vanmarcke, G., Demeke, M.M., Foulquié-Moreno, M.R., Thevelein, J.M., 2021. Identification of the major fermentation inhibitors of recombinant 2G yeasts in diverse lignocellulose hydrolysates. Biotechnol. Biofuels 14, 92. https://doi.org/10.1186/s13068-021-01935-9.

Wang, Z.-W., Zhu, M.-Q., Li, M.-F., Wang, J.-Q., Wei, Q., Sun, R.-C., 2016. Comprehensive evaluation of the liquid fraction during the hydrothermal treatment of rapeseed straw. Biotechnol. Biofuels 9, 142. https://doi.org/10.1186/s13068-016-0552-8.

Yue, P., Hu, Y., Tian, R., Bian, J., Peng, F., 2022. Hydrothermal pretreatment for the production of oligosaccharides: A review. Bioresour. Technol. https://doi.org/10.1016/j.biortech.2021.126075.

Zago, E., Tillier, C., de Leener, G., Nandasiri, R., Delporte, C., Bernaerts, K.V., Shavandi, A., 2022. Sustainable production of low molecular weight phenolic compounds from Belgian Brewers' spent grain. Bioresour. Technol. Rep. 17, 100964 https://doi.org/10.1016/j.biteb.2022.100964.

Zhuang, X., Wang, W., Yu, Q., Qi, W., Wang, Q., Tan, X., Zhou, G., Yuan, Z., 2016. Liquid hot water pretreatment of lignocellulosic biomass for bioethanol production accompanying with high valuable products. Bioresour. Technol. https://doi.org/10.1016/j.biortech.2015.08.051.